

Reaction Modeling from Molecular Dynamics Simulations

I. INTRODUCTION

The presence of the variety of degrees of freedom leads to a wide range of time scales of molecular motions. Because the size of the time step used in molecular dynamics (MD) simulations is limited by the shortest period to motion present, simulations of long time scale behavior are computationally expensive, if not impractical. For example, one may be interested in studying the slower modes in a system (e.g. torsional conformation interconversion) which necessitates a relatively long simulation time. Unfortunately, the upper limit imposed on the simulation time step by the presence of the fast modes, including bond-stretch and bond-angle changes, implies that a large number of short time steps is required to perform such a long simulation, thereby creating a major computational expense. Substantial improvement in efficiency can be achieved by freezing the fast modes, such as bond-stretching and possible bond-angle vibrations, by constraining the appropriate hard, i.e. high frequency, degrees of freedom [12].

Throughout this overview special abbreviations and terms are used. The symbol $\{\}$ denotes either a set or a subset of quantities. For example, $\{\lambda\}$ represents $\lambda_1, \lambda_2, \dots, \lambda_l$. $f^{(n)}$ denotes an n th-order derivative with respect to time of f , whereas f^n denotes an n th power of f . A single dot on top of a parameter denotes the first derivative with respect to time of that parameter and double dot denotes the second derivative with respect to time.

II. HOLONOMIC CONSTRAINT

A general holonomic constraint is defined as an algebraic equation connecting coordinates of particles and in general also time. Consider a system of N interacting particles and l general holonomic constraints that are given by

$$\sigma_k(\{\mathbf{r}(t)\}) = 0 \quad , k = 1, \dots, l. \quad (1)$$

In Eq. (1), $\{\mathbf{r}(t)\}$ denotes the subset of coordinates of the N particles involved in the particular constraint σ_k at time t . The equations of motion (EOM) for the particles are, generalized to l independent constraints,

$$\begin{aligned} \dot{\mathbf{p}}_i(t) &= \mathbf{F}_i(t) + \mathbf{G}_i(t) \\ &= -\nabla_i E_{pot}(t) - \sum_{k=1}^l \lambda_k(t) \nabla_i \sigma_k \quad , i = 1, \dots, N, \end{aligned} \quad (2)$$

where E_{pot} is the potential energy of the system, $\lambda_k(t)$ is the Lagrangian multiplier corresponding to constraint σ_k , and $\mathbf{F}_i(t)$ and $\mathbf{G}_i(t)$ denote the potential energy forces and constraint forces on site i , respectively. The forces, $\mathbf{F}_i(t)$ and $\mathbf{G}_i(t)$, depend on time implicitly through the coordinates. Eq. (1) and Eq. (2) form a set of $N + l$ equations that can be solved for the N coordinates $\{\mathbf{r}(t)\}$ and the l multipliers $\{\lambda\}$.

Lagrangian dynamics provides two approaches for dealing with systems with general holonomic constraints:

1. Within the first approach a set of independent generalized coordinates are transformed and Lagrange's equations of the first kind are used, which do not involve the forces of constraint. The equations of constraint are implicit in the transformation to independent generalized coordinates. In practice, this approach is effective only when applied to totally rigid molecular systems. It is also applicable to partially rigid molecular systems, but this method becomes increasingly complex, i.e. the choice of suitable generalized coordinates and the derivation of the EOM, as molecular size and number of constraints increase.
2. The second approach uses the Lagrange multiplier technique. A set of constrained coordinates are retained using Lagrange's equations of second kind which involve the forces constraints. Use of this approach with cartesian coordinates within molecular dynamics simulations has come to be known as constraint dynamics. This technique is equally effective for rigid and partially rigid molecular systems. In the case of totally rigid molecular systems particular care must be given to the issue of redundancy of constraints, keeping in mind that, e.g., for a non-linear system N particles the minimum number of constraints needed is $3N - 6$. Constraint dynamics is truly effective for treating partially rigid molecular systems.

The basic constraint dynamics methods employed are the analytical method and the method of undetermined parameters [12]. The analytical method includes first selecting an integration scheme (e.g. basic Verlet or velocity Verlet) requiring the input of the total forces and their derivatives with respect to time up to some order s_{max} . The forces of constraints and their derivatives with respect to time up to order s_{max} are then computed and used with the potential energy forces in the adopted integration scheme to generate the constrained coordinates. However, without the use of a correction scheme the analytical method yields constrained degrees of freedom that diverge with time from their constraint values because of the error introduced by the unavoidable numerical integration of the EOM.

The method of undetermined parameters is essentially the analytical method modified to ensure that the constraints are satisfied exactly at each time step. Basically, the modification requires that the highest derivatives with respect to time of the Lagrangian multipliers be replaced by a set of undetermined parameters with values to be determined such that the constraints are satisfied exactly at each time step. This algorithm does not introduce into the trajectories additional numerical errors any worse than the error already present in the integration scheme itself.

Most researchers are interested in the implementation of the method of undetermined parameters with different integration algorithms (e.g. basic Verlet, velocity Verlet), with holonomic constraints of various types (e.g. bond-stretch, angle-bond and torsional constraints) and with particular techniques of solution (e.g. the matrix method, SHAKE, RATTLE and SETTLE).

III. THE METHOD OF UNDETERMINED PARAMETERS

A truncated Taylor series solution of Eq. (2) yields the time derivatives of the coordinates of any order $n \geq 2$ in terms of the forces $\{\mathbf{F}(t)\}$ and their derivatives and the unknown Lagrangian multipliers $\{\lambda(t)\}$ and their derivatives:

$$\begin{aligned} \mathbf{r}_i(t + \delta t, \{\lambda^{(p)}(t)\}) &= \mathbf{r}_i(t) + \mathbf{v}_i(t)\delta t \\ &+ \sum_{n=2}^{s_{max}+2} \frac{1}{m_i} \mathbf{F}_i^{(n-2)}(t) \frac{\delta t^n}{n!} \\ &+ \sum_{n=2}^{s_{max}+2} \frac{1}{m_i} \left[\sum_{k=1}^l \sum_{p=0}^{n-2} \binom{n-2}{p} \lambda_k^{(p)}(t) [\nabla_i \sigma_k]^{n-p-2}(t) \right] \frac{\delta t^n}{n!} \\ i &= 1, \dots, N \end{aligned} \quad (3)$$

Terms of Eq. (3) can be rearranged such that that terms with same order $\{\lambda^p(t)\}$ appear together:

$$\begin{aligned} \mathbf{r}_i(t + \delta t, \{\lambda^{(p)}(t)\}) &= \mathbf{r}_i(t) + \mathbf{v}_i(t)\delta t \\ &+ \sum_{n=2}^{s_{max}+2} \frac{1}{m_i} \mathbf{F}_i^{(n-2)}(t) \frac{\delta t^n}{n!} \\ &+ \delta \mathbf{r}_i(t + \delta t, \{\lambda^{(0)}(t)\}) \\ &+ \delta \mathbf{r}_i(t + \delta t, \{\lambda^{(1)}(t)\}) \\ &+ \delta \mathbf{r}_i(t + \delta t, \{\lambda^{(2)}(t)\}) \\ &+ \dots \\ &+ \delta \mathbf{r}_i(t + \delta t, \{\lambda^{(s_{max}-1)}(t)\}) \\ &+ \delta \mathbf{r}_i(t + \delta t, \{\lambda^{(s_{max})}(t)\}) \quad , i = 1, \dots, N, \end{aligned} \quad (4)$$

where $\delta \mathbf{r}_i(t + \delta t, \{\lambda^{(0)}(t)\})$ contains s_{max} terms linear in $\{\lambda^{(0)}(t)\}$, $\delta \mathbf{r}_i(t + \delta t, \{\lambda^{(1)}(t)\})$ contains $s_{max} - 1$ terms linear in $\{\lambda^{(1)}(t)\}$, and so on. Finally, $\delta \mathbf{r}_i(t + \delta t, \{\lambda^{(s_{max})}(t)\})$ contains a single term linear in $\{\lambda^{(s_{max})}(t)\}$.

Eq. (4) can be rewritten as follows:

$$\begin{aligned} &\mathbf{r}_i(t + \delta t, \{\lambda^{(0)}(t), \dots, \lambda^{(s_{max}-1)}(t)\} \lambda^{(s_{max})}(t)) \\ &= \mathbf{r}'_i(t + \delta t, \{\lambda^{(0)}(t), \dots, \lambda^{(s_{max}-1)}(t)\}) \\ &+ \mathbf{r}_i(t + \delta t, \{\lambda^{(s_{max})}(t)\}) \quad i = 1, \dots, N, \end{aligned} \quad (5)$$

where the partially constrained position vector $\mathbf{r}'_i(t + \delta t, \{\lambda^{(0)}(t), \dots, \lambda^{(s_{max}-1)}(t)\})$ is defined as the sum of all terms except that last in Eq. (4). In the case of $s_{max} = 0$, as encountered, for example, when a basic Verlet or velocity Verlet integration algorithm is employed, $\mathbf{r}'_i(t + \delta t, \{\lambda^{(0)}(t), \dots, \lambda^{(s_{max}-1)}(t)\})$ reduces to the purely unconstrained position vector. In the first stage

of the method of undetermined parameters the set $\{\mathbf{r}'_i(t + \delta t, \{\lambda^{(0)}(t), \dots, \lambda^{(s_{max}-1)}(t)\})\}$ is evaluated by computing only $\{\lambda^{(p)}(t)\}$, where $p = 0, 1, \dots, (s_{max} - 1)$, and integrating the EOM. In the second stage the set $\{\delta \mathbf{r}\}$ are chosen to enforce the exact satisfaction of the constraints at every time step. In other words, the set $\{\lambda^{(s_{max})}(t)\}$ are replaced by a new set of parameters $\{\gamma\}$:

$$\begin{aligned} &\mathbf{r}_i(t + \delta t, \{\lambda^{(0)}(t), \dots, \lambda^{(s_{max}-1)}(t), \gamma\}) \\ &= \mathbf{r}'_i(t + \delta t, \{\lambda^{(0)}(t), \dots, \lambda^{(s_{max}-1)}(t)\}) \\ &+ \delta \mathbf{r}_i(t + \delta t, \{\gamma\}) \quad , i = 1, \dots, N \end{aligned} \quad (6)$$

that are required to have values such Eq. (1) is satisfied exactly:

$$\sigma_k(\{\mathbf{r}_i(t + \delta t, \{\lambda^{(0)}(t), \dots, \lambda^{(s_{max}-1)}(t), \gamma\})\}) = 0, \quad (7)$$

$$k = 1, \dots, l.$$

In Eq. (6), $\delta \mathbf{r}_i(t + \delta t, \{\gamma\})$ is obtained by replacing $\{\lambda^{(s_{max})}(t)\}$ by $\{\gamma\}$ in the expression for $\delta \mathbf{r}_i(t + \delta t, \{\lambda^{(s_{max})}(t)\})$. The comparison of Eq. (3) with Eq. (4) yields

$$\delta \mathbf{r}_i(t + \delta t, \{\gamma\}) = -\frac{1}{m_i} \frac{\delta t^{s_{max}+2}}{(s_{max}+2)!} \sum_{k=1}^l \gamma_k \nabla_i \sigma_k(t), \quad (8)$$

$$i = 1, \dots, N.$$

Eq. (8) is the general expression for the displacements required to satisfy the constraints. From Eq. (8) it is seen that $\delta \mathbf{r}_i$ evaluated at $(t + \delta t)$ is linear in $\{\gamma\}$ and a function of $\{\mathbf{r}(t)\}$. Adoption of a particular integration algorithm and particular forms of holonomic constraints determines the value of s_{max} and the functional dependence of $\delta \mathbf{r}_i(t + \delta t, \{\gamma\})$ on $\{\mathbf{r}(t)\}$, respectively. By means of Eq. (8), Eq. (6) becomes

$$\begin{aligned} &\mathbf{r}_i(t + \delta t, \{\lambda^{(0)}(t), \dots, \lambda^{(s_{max}-1)}(t), \gamma\}) \\ &= \mathbf{r}'_i(t + \delta t, \{\lambda^{(0)}(t), \dots, \lambda^{(s_{max}-1)}(t)\}) \\ &- \frac{1}{m_i} \frac{\delta t^{s_{max}+2}}{(s_{max}+2)!} \sum_{k=1}^l \gamma_k \nabla_i \sigma_k(t) \end{aligned} \quad (9)$$

The general formalism consists of two steps: (1) the computation of the partially constrained coordinates and (2) the calculation of the undetermined parameters and constrained coordinates. Step (1) begins with the selection of a numerical algorithm to integrate the EOM. Initially, the Lagrangian multipliers and their time derivatives of the partially constrained coordinates $\{\mathbf{r}'_i(t + \delta t, \{\lambda^{(0)}(t), \dots, \lambda^{(s_{max}-1)}(t)\})\}$ must be calculated. The forces of constraint and their time derivatives up to order s_{max} are then evaluated for use in the integration scheme. The numerical integration of the EOM, Eq. (2), yields the partially constrained coordinates $\{\mathbf{r}'(t + \delta t, \{\lambda^{(0)}(t), \dots, \lambda^{(s_{max}-1)}(t)\})\}$. Using the forces $\{\mathbf{F}(t)\}$ and their time derivatives up to order s_{max} together with the forces $\{\mathbf{G}(t)\}$ and their time derivatives up to order s_{max} , the partially constrained position vectors $\{\mathbf{r}'(t + \delta t)\}$ are computed.

When $\{\mathbf{r}'(t + \delta t, \{\lambda^{(0)}(t), \dots, \lambda^{(s_{max}-1)}(t)\})\}$ are known the undetermined parameters $\{\gamma\}$ can be obtained. The most general form of holonomic constraint is nonlinear in the particle

positions. Even the simple bond-stretch constraint is nonlinear. Consequently, one has to solve a system of l coupled nonlinear equations for the l unknowns $\{\gamma\}$. These kind of equations can be solved in an iterative procedure that based on a Taylor expansion of the holonomic constraint, σ_k , and a linearization [12]. But the validity of these approximations underlying the iterative method must be carefully examined for every form of holonomic constraint, σ_k .

The calculated $\{\gamma\}$ are substituted into Eq. (8) to provide the displacements necessary to satisfy the constraints. Subsequently, the constrained position vectors, $\mathbf{r}_i(t + \delta t)$ are obtained from Eq. (??) by adding the constraint corrections to the partially constraint position vectors.

IV. THE METHOD OF UNDETERMINED PARAMETERS COMBINED WITH THE VELOCITY VERLET INTEGRATION ALGORITHM

The basic Verlet algorithm has many advantages but it suffers from a number of drawbacks:

1. A term of $o(\delta t^2)$ is added to terms of $o(\delta t^0)$ of the basic Verlet recipe in the calculation of the unconstrained coordinates $\{\mathbf{r}'(t + \delta t)\}$, leading eventually to numerical precision problems.
2. The velocities of the atoms at time t can be obtained only after the coordinates at time $(t + \delta t)$ are available, resulting in difficulties in implementing the basic Verlet algorithm in constant pressure, constant temperature and nonequilibrium MD simulations.
3. The basic Verlet algorithm is not self-starting and two successive initial configurations of the system must be provided to start the integration.

To avoid these shortcomings the velocity Verlet algorithm is incorporated into the method of undetermined parameters. Both, the basic Verlet and the velocity Verlet schemes have global errors of $o(\delta t^2)$. However, the local error of the velocity Verlet integrations is of $o(\delta t^3)$, in contrast to the local errors $o(\delta t^4)$ and $o(\delta t^2)$ of the basic Verlet integrations.

As in the basic Verlet scheme the highest derivative with respect to time of the coordinates in the velocity Verlet algorithm is of second order. Therefore, the coordinate equations of the method of undetermined parameters with the velocity Verlet scheme are

$$\mathbf{r}_i(t + \delta t, \{\gamma\}) = \mathbf{r}'_i(t + \delta t) - \frac{\delta t^2}{2m_i} \sum_{k=1}^l \gamma_k \nabla_i \sigma_k(t), \quad (10)$$

which follows from Eq. (9) with $s_{max} = 0$. The purely unconstrained position vector $\mathbf{r}'_i(t + \delta t)$ is given by

$$\mathbf{r}'_i(t + \delta t) = \mathbf{r}_i(t) + \mathbf{v}_i(t)\delta t + \mathbf{a}_i \frac{\delta t^2}{2}. \quad (11)$$

The parameters $\{\gamma\}$ are determined such that the coordinates at time $(t + \delta t)$ satisfy the constraint equations. The new velocities are

$$\begin{aligned} \mathbf{v}_i(t + \delta t, \{\eta\}) &= \mathbf{v}'_i(t + \delta t, \{\eta\}) \\ &- \frac{\delta t}{2m_i} \sum_{k=1}^l \eta_k \nabla_i \sigma_k(t + \delta t). \end{aligned} \quad (12)$$

The parameters $\{\eta\}$ are chosen such that also the velocities at time $(t + \delta t)$ satisfy the constraint equations. Taking the first derivatives with respect to time of the constraint equation for $\sigma_k(\{\mathbf{r}(t + \delta t)\})$ and applying the chain rule one obtains

$$\begin{aligned} \frac{d}{dt} \sigma_k(\{\mathbf{r}(t + \delta t)\}) &= \sum_{i=1}^{n_k} \mathbf{v}_i(t + \delta t) \cdot \nabla_i \sigma_k(\{\mathbf{r}(t + \delta t)\}) \\ &= 0 \end{aligned} \quad (13)$$

Either matrix inversion technique [12] or the SHAKE approach [12] can be used to solve the set of l linear equations Eq. (13) for $\{\eta\}$. Solutions for $\{\gamma\}$ and $\{\eta\}$ by matrix techniques become computationally expensive for systems with large number of coupled constraints. In such cases, hence, it is better to apply the SHAKE procedure. The SHAKE procedure was written for the basic Verlet integration algorithm and consists of finding incrementally the displacement a particle needs to satisfy successively all constraints imposed.

The solution for $\{\gamma\}$ and $\{\eta\}$ within the velocity Verlet integration algorithm using SHAKE is termed RATTLE. The first stage of RATTLE is analogous to SHAKE. The new positions of the particles $\{\mathbf{r}^{new}(t + \delta t)\}$ obtained in the current iteration is

$$\begin{aligned} \mathbf{r}_i^{new}(t + \delta t) &= \mathbf{r}_i^{old}(t + \delta t) \\ &- \frac{\delta t^2}{2m_i} \gamma_k^{new} \nabla_i \sigma_k(t), \quad i = 1, \dots, n_k \end{aligned} \quad (14)$$

where the starting value of $\mathbf{r}_i^{old}(t + \delta t)$ is given by Eq. (11). The new positions should satisfy the constraint equation for σ_k ,

$$\begin{aligned} \sigma_k(\{\mathbf{r}^{new}(t + \delta t)\}) &= \sigma_k \left(\{\mathbf{r}^{old}(t + \delta t)\} - \left\{ \frac{\delta t^2}{m} \gamma_k^{new} \nabla \sigma_k(t) \right\} \right) \\ &= 0. \end{aligned} \quad (15)$$

Eq. (15) is generally nonlinear in γ_k^{new} , even in the common case of a bond-stretch constraint. After a Taylor expansion of each holonomic constraint $\sigma_k(\{\mathbf{r}^{new}(t + \delta t)\})$ around $\{\mathbf{r}^{old}(t + \delta t)\}$, Eq. (15) becomes

$$\begin{aligned} \sigma_k \left(\{\mathbf{r}^{old}(t + \delta t)\} - \left\{ \frac{\delta t^2}{m} \gamma_k^{new} \nabla \sigma_k(t) \right\} \right) &= \\ \sigma_k(\{\mathbf{r}^{old}(t + \delta t)\}) & \\ - \sum_{i=1}^{n_k} \frac{\delta t^2}{m_i} \gamma_k^{new} \nabla_i \sigma_k(t) \cdot \nabla_i \sigma_k(\{\mathbf{r}^{old}(t + \delta t)\}) & \\ + \dots &= 0, \end{aligned} \quad (16)$$

where the nonlinear terms are not shown explicitly. For every particular form of holonomic constraint, σ_k , the domain of

validity of the Taylor representation in Eq. (16) needs to be carefully established.

For computationally efficiency, all terms higher than first order in Eq. (16) are neglected because the iterative process over constraints ensures that the solution obtained in this manner will satisfy the nonlinear Eq. (16). Solving Eq. (16) for γ_k^{new} , one obtains

$$\gamma_k^{new} = \frac{1}{\delta t^2} \frac{\sigma(\{\mathbf{r}^{old}(t + \delta t)\})}{\sum_{i=1}^{n_k} (1/2m_i) \nabla_i \sigma_k(t) \cdot \nabla_i \sigma_k(\{\mathbf{r}^{old}(t + \delta t)\})} \quad (17)$$

The validity of neglecting all nonlinear terms in Eq. (16) must be carefully examined for every form of holonomic constraint, σ_k , and the larger the nonlinearity inherent in the constraint, σ_k , the smaller the allowed size of the constraint corrections to justify neglecting the nonlinear terms.

Iterations over the constraints continue until all are satisfied, within a certain tolerance. When all constraints have been satisfied and the coordinates at $(t + \delta t)$ are available, the forces $\{\mathbf{F}(t + \delta t)\}$ can be computed for use in the second stage of RATTLE. In the second stage, the new velocities of the particles $\{\mathbf{v}^{new}(t + \delta t)\}$ obtained in the current iteration are

$$\mathbf{v}_i^{new}(t + \delta t) = \mathbf{v}_i^{old}(t + \delta t) - \frac{\delta t}{2m_i} \eta_k^{new} \nabla_i \sigma_k(t + \delta t), \quad i = 1, \dots, n_k, \quad (18)$$

where the starting value of $\mathbf{v}_i^{old}(t + \delta t)$ is given by

$$\mathbf{v}_i'(t + \delta t) = \mathbf{v}_i(t) + \frac{\delta t}{2m_i} \left[\mathbf{F}_i(t) - \sum_{k=1}^l \nabla_i \sigma_k(t) + \mathbf{F}_i(t + \delta t) \right] \quad (19)$$

The new velocities should satisfy the derivative with respect to time of the constraint equation. Inserting Eq. (18) into Eq. (13) yields

$$\begin{aligned} & \sum_{i=1}^{n_k} \mathbf{v}_i^{old}(t + \delta t) \cdot \nabla_i \sigma_k(\{\mathbf{r}(t + \delta t)\}) \\ & - \eta_k^{new} \sum_{i=1}^{n_k} \frac{\delta t}{2m_i} \nabla_i \sigma_k(\{\mathbf{r}(t + \delta t)\}) \cdot \nabla_i \sigma_k(\{\mathbf{r}(t + \delta t)\}) \\ & = 0 \end{aligned} \quad (20)$$

The solution of this linear equation for η_k^{new} is

$$\eta_k^{new} = \frac{1}{\delta t} \frac{\sum_{i=1}^{n_k} \mathbf{v}_i^{old}(t + \delta t) \cdot \nabla_i \sigma_k(\{\mathbf{r}(t + \delta t)\})}{\sum_{i=1}^{n_k} (1/2m_i) \nabla_i \sigma_k(\{\mathbf{r}(t + \delta t)\}) \cdot \nabla_i \sigma_k(\{\mathbf{r}(t + \delta t)\})} \quad (21)$$

Again, iterations over all constraints continues until the constraints on the velocities have been satisfied within a selected tolerance. The entire procedure is repeated at the next time step.

A. Application to bond-stretch constraint

Consider a system of N particles and l general holonomic constraints and assume that l_s bond-stretch constraints ($l_s \leq l$)

are present. For bond-stretch constraints the general holonomic constraint, Eq. (1), takes the special form

$$\sigma_k(\{\mathbf{r}\}) = [\mathbf{r}_i(t) - \mathbf{r}_j(t)]^2 - d_{ij}^2 = \mathbf{r}_{ij}^2(t) - d_{ij}^2 = 0, \quad k = 1, \dots, l_s, \quad (22)$$

where i and j are the particles involved in the particular constraint, σ_k , and d_{ij} is the constant distance between the (ij) pair of particles.

For bond-stretch constraints and the first stage of RATTLE, inserting the constraint $\sigma_k(\{\mathbf{r}\})$ of Eq. (22) into Eq. (14) yields

$$\begin{aligned} \mathbf{r}_j^{new}(t + \delta t) &= \mathbf{r}_j^{old}(t + \delta t) - \frac{1}{m_j} \delta t^2 \gamma_k^{new} [\mathbf{r}_j(t) - \mathbf{r}_i(t)] \\ \mathbf{r}_i^{new}(t + \delta t) &= \mathbf{r}_i^{old}(t + \delta t) - \frac{1}{m_i} \delta t^2 \gamma_k^{new} [\mathbf{r}_i(t) - \mathbf{r}_j(t)] \end{aligned} \quad (23)$$

and Eq. (17) reduces to

$$\begin{aligned} \gamma_k^{new} &= \frac{1}{\delta t^2} \\ & \times \frac{[\mathbf{r}_j^{old}(t + \delta t) - \mathbf{r}_i^{old}(t + \delta t)]^2 - d_{ij}^2}{2[(1/m_i) + (1/m_j)][\mathbf{r}_j(t) - \mathbf{r}_i(t)][\mathbf{r}_j^{old}(t + \delta t) - \mathbf{r}_i^{old}(t + \delta t)]} \\ & \quad k = 1, \dots, l_s. \end{aligned} \quad (24)$$

The iteration procedure is assumed to have converged when [16]

$$\frac{|\mathbf{r}_{ij}^2(t) - d_{ij}^2|}{2d_{ij}^2} \approx \frac{|\mathbf{r}_{ij}(t) - d_{ij}|}{d_{ij}^2} < \tau, \quad (25)$$

where τ is the tolerance criteria.

For the second stage of RATTLE, Eq. (18) becomes

$$\begin{aligned} \mathbf{v}_j^{new}(t + \delta t) &= \mathbf{v}_j^{old}(t + \delta t) \\ & - \frac{1}{m_j} \delta t \eta_k^{new} [\mathbf{r}_j(t + \delta t) - \mathbf{r}_i(t + \delta t)] \\ \mathbf{v}_i^{new}(t + \delta t) &= \mathbf{v}_i^{old}(t + \delta t) \\ & - \frac{1}{m_i} \delta t \eta_k^{new} [\mathbf{r}_i(t + \delta t) - \mathbf{r}_j(t + \delta t)] \end{aligned} \quad (26)$$

and Eq. (21) reduces to

$$\eta_k^{new} = \frac{1}{\delta t} \frac{[\mathbf{r}_j(t + \delta t) - \mathbf{r}_i(t + \delta t)][\mathbf{v}_j^{old}(t + \delta t) - \mathbf{v}_i^{old}(t + \delta t)]}{[(1/m_i) + (1/m_j)][\mathbf{r}_j(t + \delta t) - \mathbf{r}_i(t + \delta t)]^2} \quad k = 1, \dots, l_s \quad (27)$$

Because the coordinates at $(t + \delta t)$ from the first stage satisfy (to within a given tolerance) the constraint Eq. (22), Eq. (27) can be rewritten as follows:

$$\eta_k^{new} = \frac{1}{\delta t} \frac{[\mathbf{r}_j(t + \delta t) - \mathbf{r}_i(t + \delta t)][\mathbf{v}_j^{old}(t + \delta t) - \mathbf{v}_i^{old}(t + \delta t)]}{[(1/m_i) + (1/m_j)]d_{ij}^2} \quad k = 1, \dots, l_s \quad (28)$$

The iteration procedure is assumed to have converged when [16]

$$\frac{1}{d_{ij}^2} |[\mathbf{r}_j(t + \delta t) - \mathbf{r}_i(t + \delta t)][\mathbf{v}_j^{old}(t + \delta t) - \mathbf{v}_i^{old}(t + \delta t)]| \delta t < \tau \quad (29)$$

where τ is the tolerance criteria.

B. Application to angle-bend constraints

Again, consider a system of N particles and l general holonomic constraints and assume that l_a angle-bend constraints ($l_a \leq l$) are present. For angle-bend constraints the general holonomic constraint, Eq. (1), takes the special form

$$\sigma_k(\{\mathbf{r}\}) = \theta_{abc}(\{\mathbf{r}\}) - \alpha_{abc} = 0 \quad , k = 1, \dots, l_a, \quad (30)$$

where a, b and c are three particles involved in the particular constraint σ_k , $\theta_{abc} \equiv \arccos(\hat{\mathbf{r}}_{ab} \cdot \hat{\mathbf{r}}_{cb})$ is the angle at b formed by the abc triplet of particles, $\hat{\mathbf{r}}_{ab} \equiv \mathbf{r}_{ab}/|\mathbf{r}_{ab}|$, $\mathbf{r}_{ab} \equiv \mathbf{r}_a - \mathbf{r}_b$ and α_{abc} is the constant constraint angle-bend value.

For angle-bend constraints and the first stage of RATTLE, inserting the constraint $\sigma_k(\{\mathbf{r}\})$ of Eq. (30) into Eq. (14) yields

$$\mathbf{r}_i^{new}(t + \delta t) = \mathbf{r}_i^{old}(t + \delta t) - \frac{\delta t^2}{2m_i} \gamma_k^{new} \nabla_i \theta_{abc}(t) \quad , i = a, b, c, \quad (31)$$

and Eq. (17) reduces to

$$\gamma_k^{new} = \frac{1}{\delta t^2} \frac{\theta_{abc}(\{\mathbf{r}^{old}(t + \delta t)\}) - \alpha_{abc}}{\sum_{i=1}^{n_k} (1/2m_i) \nabla_i \theta_{abc}(t) \cdot \nabla_i \theta_{abc}(\{\mathbf{r}^{old}(t + \delta t)\})} \quad , k = 1, \dots, l_a \quad (32)$$

The iteration procedure is assumed to have converged when [16]

$$\frac{|\theta_{abc}(\{\mathbf{r}(t + \delta t)\}) - \alpha_{abc}|}{\alpha_{abc}} < \tau \quad , \quad (33)$$

where τ is the tolerance criteria.

For the second stage of RATTLE, Eq. (18) becomes

$$\mathbf{v}_i^{new}(t + \delta t) = \mathbf{v}_i^{old}(t + \delta t) - \frac{\delta t}{2m_i} \eta_k^{new} \nabla_i \theta_{abc}(\{\mathbf{r}(t + \delta t)\}) \quad , i = a, b, c \quad (34)$$

and Eq. (21) reduces to

$$\eta_k^{new} = \frac{1}{\delta t} \frac{\sum_{i=1}^{n_k} \mathbf{v}_i^{old}(t + \delta t) \cdot \nabla_i \theta_{abc}(\{\mathbf{r}(t + \delta t)\})}{\sum_{i=1}^{n_k} (1/2m_i) [\nabla_i \theta_{abc}(\{\mathbf{r}(t + \delta t)\})]^2} \quad , k = 1, \dots, l_a. \quad (35)$$

The iteration procedure is assumed to have converged when [16]

$$\frac{|\sum_{i=1}^{n_k} \mathbf{v}_i(t + \delta t) \cdot \nabla_i \theta_{abc}(\{\mathbf{r}(t + \delta t)\})| \delta t}{\alpha_{abc}} < \tau \quad . \quad (36)$$

where τ is the tolerance criteria.

C. Application to torsional constraints

Consider a system of N particles and l general holonomic constraints and assume that l_t torsional constraints ($l_t \leq l$) are

present. For torsional constraints the general holonomic constraint, Eq. (1), takes the special form

$$\sigma_k(\{\mathbf{r}\}) = \tau_{abcd}(\{\mathbf{r}\}) - \beta_{abcd} = 0 \quad , k = 1, \dots, l_t, \quad (37)$$

where a, b, c and d are the four particles involved in the particular constraint, σ_k , and

$$\tau_{abcd} \equiv \arccos \left[\frac{(\hat{\mathbf{r}}_{ab} \times \hat{\mathbf{r}}_{cb}) \cdot (\hat{\mathbf{r}}_{bc} \times \hat{\mathbf{r}}_{dc})}{\sin \theta_{abc} \sin \theta_{bcd}} \right] \quad (38)$$

is the dihedral angle formed by the $abcd$ quadruple of particles. The parameter β_{abcd} is the constant constraint value of τ_{abcd} .

For torsional constraints and the first stage of RATTLE, inserting the constraint $\sigma_k(\{\mathbf{r}\})$ of Eq. (37) into Eq. (14) yields

$$\begin{aligned} \mathbf{r}_i^{new}(t + \delta t) &= \mathbf{r}_i^{old}(t + \delta t) \\ &- \frac{\delta t^2}{2m_i} \gamma_k^{new} \nabla_i \tau_{abcd}(t) \quad , i = a, b, c, d, \end{aligned} \quad (39)$$

and Eq. (17) reduces to

$$\gamma_k^{new} = \frac{1}{\delta t^2} \frac{\tau_{abcd}(\{\mathbf{r}^{old}(t + \delta t)\}) - \beta_{abcd}}{\sum_{i=1}^{n_k} (1/2m_i) \nabla_i \tau_{abcd}(t) \cdot \nabla_i \tau_{abcd}(\{\mathbf{r}^{old}(t + \delta t)\})} \quad , k = 1, \dots, l_t. \quad (40)$$

The iteration procedure is assumed to have converged when [16]

$$\frac{|\tau_{abcd}(\{\mathbf{r}(t + \delta t)\}) - \beta_{abcd}|}{\beta_{abcd}} < \tau \quad , \quad (41)$$

where τ is the tolerance criteria.

For the second stage of RATTLE, Eq. (18) becomes

$$\begin{aligned} \mathbf{v}_i^{new}(t + \delta t) &= \mathbf{v}_i^{old}(t + \delta t) \\ &- \frac{\delta t}{2m_i} \eta_k^{new} \nabla_i \tau_{abcd}(\{\mathbf{r}(t + \delta t)\}) \quad , i = a, b, c, d, \end{aligned} \quad (42)$$

and Eq. (21) reduces to

$$\eta_k^{new} = \frac{1}{\delta t} \frac{\sum_{i=1}^{n_k} \mathbf{v}_i^{old}(t + \delta t) \cdot \nabla_i \tau_{abcd}(\{\mathbf{r}(t + \delta t)\})}{\sum_{i=1}^{n_k} (1/2m_i) [\nabla_i \tau_{abcd}(\{\mathbf{r}(t + \delta t)\})]^2} \quad , k = 1, \dots, l_t. \quad (43)$$

The iteration procedure is assumed to have converged when [16]

$$\frac{|\sum_{i=1}^{n_k} \mathbf{v}_i(t + \delta t) \cdot \nabla_i \tau_{abcd}(\{\mathbf{r}(t + \delta t)\})| \delta t}{\beta_{abcd}} < \tau \quad . \quad (44)$$

where τ is the tolerance criteria.

The global error of RATTLE is of $o(\delta t^2)$ which is the same as for the SHAKE algorithm.

V. NUMERICAL DIFFICULTIES WITHIN THE SHAKE/RATTLE SCHEMES

If during SHAKE or RATTLE iterations it happens that

$$\nabla_i \sigma_k(t) \perp \nabla_i \sigma_k(\{\mathbf{r}^{old}(t + \delta t)\}) \quad , i = 1, \dots, n_k \quad (45)$$

a singularity occurs in Eq. (17) because each dot product in the denominator is zero. In that case, a solution using SHAKE is impossible. Eq. (45) states that the SHAKE displacements are orthogonal to the corresponding displacements that produce maximum change in the molecular configuration $\{\mathbf{r}^{old}(t + \delta t)\}$. Clearly, such SHAKE displacements have no effect on the molecular configuration $\{\mathbf{r}^{old}(t + \delta t)\}$ and in particular cannot lead to a new configuration $\{\mathbf{r}^{new}(t + \delta t)\}$.

VI. NON-ITERATIVE CONSTRAINT MD USING THE VELOCITY VERLET METHOD

The most widely used numerical methods for determining constraint forces are the SHAKE and RATTLE algorithms (an overview provides Ref. [12]). However, when implemented on parallel computer architecture such iterative algorithms can give rise to difficulties with load balancing as well as vectorization and parallelization. To avoid these problems a non-iterative method would therefore be highly advantageous.

Such an algorithm within the framework of the velocity Verlet scheme for bond-stretch constraints were suggested by Slusher and Cummings [18]. The velocity Verlet algorithm can be implemented in a constraint dynamics scheme when the particle forces calculated at the previous time step will already include the correct constraint forces necessary to ensure the position updates to satisfy Eq. (22). Hence, the apparent problem arises in evaluating the new velocities, $\{\mathbf{v}(t + \delta t)\}$. However, this problem can be avoided by writing the position update, Eq. (11) in terms of the *previous* velocities:

$$\mathbf{v}'(t) = \mathbf{v}'(t - \delta t) + \frac{\delta t}{2} [\mathbf{a}(t - \delta t) + \mathbf{a}(t)] \quad , i = 1, \dots, l_s. \quad (46)$$

The substitution of Eq. (46) into Eq. (11) yields for the distance between a (ij) pair of particles

$$\begin{aligned} \mathbf{r}_{ij}(t + \delta t) = & \mathbf{r}_{ij}(t) + \mathbf{v}_{ij}(t - \delta t)\delta t \\ & + \mathbf{a}_{ij}(t - \delta t)\frac{\delta t^2}{2} + \mathbf{a}_{ij}(t)\delta t^2. \end{aligned} \quad (47)$$

Using Eq. (47) in Eq. (22) yields an expression for $\sigma_k(t + \delta t)$ linear in $\gamma_k(t)$ that is accurate in third order:

$$\begin{aligned} \sigma(t + \delta t) = & \mathbf{r}_{ij}^2(t) - d_{ij}^2 + 2\mathbf{r}_{ij}(t) \cdot \mathbf{v}_{ij}(t - \delta t)\delta t \\ & + \mathbf{v}_{ij}(t - \delta t)\delta t^2 \\ & + \{\mathbf{r}_{ij}(t) + \delta t^2 \mathbf{v}_{ij}(t - \delta t)\} \\ & \cdot \{2\mathbf{a}_{ij}(t) + \mathbf{a}_{ij}(t - \delta t)\} \delta t^2 \\ & + o(\delta t^4) = 0 \end{aligned} \quad (48)$$

Within the velocity Verlet algorithm, Eq. (48) can be applied immediately after the position update and force evaluation.

This allows the same constraint forces to be used in both the position and velocity updates. Substituting the constrained EOM for $\mathbf{a}_{ij}(t)$ in Eq. (48) gives a rank M matrix which can be solved using, e.g., LAPACK routines. Note, Eq. (48) contains quantities which are unknown at the start of the simulation, i.e. at $(t - \delta t)$. In practice these can be set to zero at startup until they have been accumulated.

VII. TRANSITION STATE SEARCH

Determining transition states is the key to understanding reaction mechanisms. One method to locate transition states uses constraint (external) forces, such as defined by a holonomic constraint, Eq. (2), to move a system “up-hill” towards a transition state and to stabilize the system at the transition state. The imposed constraint closely resembles the reaction coordinate.

As an example, the constraint chosen for a simple bond-breaking or bond-forming reaction between two atoms A and B would have the form of Eq. (22). The value of the reaction coordinate, d_{AB} , is continuously varied with time so that the system proceeds from the initial configuration to the transition state.

While the system moves from the initial configuration across the barrier, all atoms are free to relax under the given constraint. If the motion was sufficiently slow, the exact transition state would be obtained as the maximum of the potential energy as a function of the reaction coordinate. In practice, however, the ascent to the transition state is too fast for keeping all degrees of freedom relaxed. Therefore, the value of the constraint is fixed at the maximum of the potential energy and the system is relaxed fully under this condition. The constraint force will now have a finite value, whose sign indicates on which side of the barrier the calculation has stopped. Then the transition state search is continued from the this point onward. This iterative procedure has converged when the force acting on the constraint is sufficiently small. Finally, the position of the transition state is refined by interpolating energy and constraint force from the last few relaxation steps.

A transition state is definitely reached when all forces obtained vanish and that there is exactly one imaginary vibrational frequency. Obviously, the forces vanish: The system is fully relaxed under the constraint condition, that is all forces perpendicular to the reaction coordinate vanish. As the energy is maximized along the reaction coordinate, also the force acting in parallel to the reaction coordinate vanishes.

In order to show there is exactly one imaginary vibrational frequency the potential energy, E , is expanded up to second order in the deviation from the transition state at $\mathbf{r}_{i,T}$ and the

constraint, σ , is expanded up to first order [2].

$$\begin{aligned}
 E(\{\mathbf{r}\}) &= E_T & (49) \\
 &+ \frac{1}{2} \sum_{i,j} (\mathbf{r}_i - \mathbf{r}_{i,T}) \Delta_{i,j} E(\mathbf{r}_j - \mathbf{r}_{j,T}) \\
 &+ o[(\mathbf{r}_j - \mathbf{r}_{j,T})^3] \\
 \sigma(\{\mathbf{r}\}) &= \sum_{i,j} b_i (\mathbf{r}_i - \mathbf{r}_{i,T}) + o[(\mathbf{r}_j - \mathbf{r}_{j,T})^2], & (50)
 \end{aligned}$$

where E_T is the energy of the transition state. The reason for going only to first order in the constraint lies in the fact that the constraint forces are multiplied by the Lagrange parameters, which depend themselves to first order on the deviation from the transition state.

The EOM near the transition state are

$$\mathbf{p}_i = - \sum_j \Delta_{i,j} E(\mathbf{r}_j - \mathbf{r}_{j,T}) + b_i \lambda, \quad (51)$$

where $b_i \lambda = (\partial \sigma / \partial \mathbf{r}_i) \lambda$ is the force of constraint.

A variable transformation simplifies these EOM to

$$\ddot{S}_i = - \sum_j D_{i,j} S_j + B_i \lambda, \quad (52)$$

where $S_i = \sqrt{m_i} (\mathbf{r}_i - \mathbf{r}_{i,T})$, $\Delta_{i,j} E / \sqrt{m_i m_j}$ is the dynamical matrix, and $B_i = b_i / \sqrt{m_i}$ is the transformed constraint vector. The eigenvalues of the dynamical matrix are the squared frequencies and the eigenvectors divided by the square-root of the masses are the vibrational eigenmodes.

As the energy of the transition state is a local maximum along the reaction coordinate, the dynamical matrix cannot be positive definite, so it must contain at least one negative eigenvalue, i.e., one imaginary vibrational frequency.

If there were more than one imaginary vibrational frequency, at least two eigenvectors U and V of the dynamical matrix have negative eigenvalues of which at least one has a projection onto \mathbf{B} . Taking into account this assumption one can show that such a system is unstable and does not result in a solution of the transition state search. Out of these two vectors at least one vector $W_i = U_i \sum_j V_j B_j - V_i \sum_j U_j B_j$ can be constructed that is orthogonal to \mathbf{B} . This vector lies within the constraint hypersurface. Evaluating the energy along this direction, that is for $S_i = \alpha W_i$, where α is an arbitrary small parameter, it is negatively curved, hence the system is unstable. When the system is relaxed along all unconstrained distortions, the system will therefore move away from such a state.

A converged result can thus only be obtained for the true transition state with exactly one negative eigenvalue, i.e. one imaginary vibrational frequency.

The constraints used to find reaction barriers need to fulfill the requirement that they do not have any projection onto translation or rotation of the molecule as a whole. If this is the case, any value of the constraint could be reached in the ground state by translating or rotating the molecule. One remedy is to define the constraints in terms of relative coordinates, such as bond lengths, bond angles, etc. Another solution is to impose additional constraints that prohibit any translation or rotation of the molecule.

VIII. DYNAMICAL REACTION PATH AND INTRINSIC REACTION COORDINATE

Once the transition state has been located the reaction path is interesting. Reactions at finite temperature pass the barrier in a variety of ways. In an attempt to single out one particular path, the so-called ‘‘intrinsic reaction coordinate’’ (IRC) has been defined. The IRC is obtained from $\mathbf{p}_i = -\partial E[\{\mathbf{r}\}] / \partial \mathbf{r}_i$.

But there are other possible definitions of a reaction pathway. The ‘‘dynamical reaction path’’ (DRP) is the zero-temperature limit. The DRP is also known as ‘‘dynamical reaction coordinate’’ (DRC). The rationale behind the definition of the DRP is as follows: Consider an arbitrarily low temperature. In this case the reaction is a very rare event. However, if only those trajectories are monitored that cross the barrier, the trajectories become increasingly similar to each other as the temperature is lowered. In the limit, this path will pass with probability one through the exact saddle point with zero velocity.

The DRP is obtained in practice by first determining the saddle point of the potential energy surface. Then, two trajectories, obeying Newton’s EOM, are created, starting from the saddle point with arbitrarily small velocity. One of the trajectories is reversed in time and the two paths are joined at the saddle point. The DRP corresponds to a system at $T = 0$ K with negligible coupling to the heat bath.

On the other hand, the IRC approach corresponds to a system at $T = 0$ K with strong coupling to the heat bath, such that the excess kinetic energy, produced while descending from the barrier, is instantaneously dissipated. Both methods can therefore be considered as two limiting cases of a $T = 0$ K approach. The zero-temperature limit is reasonably justified if the reaction barrier is large compared to thermal energies. This approximation serves to give a unique definition of the reaction path.

The DRP has the advantage that it would represent the true dynamics at zero temperature, if the heat bath is explicitly included in the calculations. The DRP has relevance also at higher temperatures, in the sense that it is the most probable path across the barrier. It has, however, the disadvantage that it does not directly approach the ground state but maintains the reaction energy indefinitely. The reaction energy is dissipated only infinitely slowly due to the infinitesimal coupling to the heat bath. Correctly formulated, the DRP corresponds to a microcanonical (NVE) ensemble.

It is conceivable to extend this approach to an intermediate coupling which would correspond to applying a constant friction that reflected the heat transfer from a molecule to the environment and that were proportional to the atomic masses and a scaling factor estimated from the heat equation.

IX. ZERO TEMPERATURE TECHNIQUES

Within zero temperature approaches finite temperature reaction enthalpies at a temperature T and the entropies are es-

estimated using [7]

$$\Delta H_T = \Delta E_{pot} + \Delta E_{ZPE} \quad (53)$$

$$+ \Delta E_T^v + \Delta E_T^r + \Delta E_T^t + \Delta(PV)$$

$$\Delta S = R \ln(Q_{trans} Q_{rot} Q_{vib}) \quad (54)$$

with E_{pot} being the sum of the electronic energy in a static nuclear field (Born-Oppenheimer approximation) and the nuclear electrostatic repulsion. The zero-point vibrational energy, E_{ZPE} , and the temperature-dependent vibrational energy, E_T^v , are obtained from calculations of harmonic vibrational frequencies using, e.g., density functional methods. The change in translational energy, ΔE_T^t , rotational energy, ΔE_T^r and PV are approximated using the ideal gas law, associating $1/2k_B T$ to each degree of freedom, where k_B is the Boltzmann constant. The partition functions Q is the product of translational, rotational and vibrational contributions (see e.g. chapter 20 in Ref. [1] and Sec. XI).

X. FINITE TEMPERATURE SIMULATIONS

Simulations at finite temperature offer additional ways to study chemical reactions. Besides making true finite temperature quantities such as entropies of reaction accessible, these simulations are a tool to explore phase space in an unbiased and more effective way than it is possible at zero temperature. The most straightforward and most unbiased approach is a finite-temperature simulation of the system, monitoring the frequency with which the reaction takes place [2]. This approach is best when the barriers are low or the temperatures sufficiently large so that a significant number of reaction events can be observed in a simulation of typically 5–20 ps, needed to obtain a reasonably small statistical error bar.

On the other hand, when the barriers are large, techniques other than direct simulations are more appropriate. The zero-temperature transition state search can be extended to finite temperatures. A number of special methodologies have been developed to calculate relative free energies. One approach to calculate reaction free energy barriers and activation energies along a reaction path defined by varying a reaction coordinate ϕ is known as the ‘‘blue moon ensemble’’, a kind of thermodynamic integration [3, 5, 19]. Here the integration variable is the reaction coordinate which, however, is not an independent parameter of the Hamiltonian but a function $\phi = \phi(\mathbf{r})$ of the configurational degrees of freedom \mathbf{r} . The free energy difference, ΔA , between an initial state at ϕ_1 and a final state ϕ_2 , of a statistical ensemble is given by [19]

$$\begin{aligned} \Delta A_{(\phi_1 \rightarrow \phi_2)} &= A(\phi_2) - A(\phi_1) \\ &= \int_{\phi_1}^{\phi_2} \left\langle \frac{\partial E_{pot}(\phi)}{\partial \phi} \right\rangle_{\phi'}^{\text{cond.}} d\phi' \quad (55) \\ &= \int_{\phi_1}^{\phi_2} F(\phi') d\phi' \end{aligned}$$

In Eq. (55), superscript and subscript are added to indicate that the integrand is a conditional ensemble average evaluated

at $\phi(\mathbf{r}) = \phi'$:

$$\langle \dots \rangle_{\phi'}^{\text{cond.}} = \frac{\langle \dots \delta(\phi(\mathbf{r} - \phi')) \rangle}{\langle \delta(\mathbf{r} - \phi') \rangle}. \quad (56)$$

The mean force $F(\phi')$ is calculated with [19]

$$F(\phi') = \frac{\langle Z^{-1/2} [-\lambda + k_B T G] \rangle_{\phi'}^{\text{cond.}}}{\langle Z^{-1/2} \rangle_{\phi'}^{\text{cond.}}}, \quad (57)$$

where the term G is defined by

$$G = \frac{1}{Z^2} \sum_{i=1}^N \sum_{j=1}^N \frac{1}{m_i m_j} \frac{\partial \phi}{\partial \mathbf{r}_i} \frac{\partial^2 \phi}{\partial \mathbf{r}_i \partial \mathbf{r}_j} \frac{\partial \phi}{\partial \mathbf{r}_j}. \quad (58)$$

The parameter λ appearing in Eq. (57) is identical to the Lagrange undetermined multiplier obtained by solving the EOM in Cartesian coordinates (Sec. IV). The term Z in Eqs. (57) and (58) serves to remove the bias generated by the constrained MD trajectory. The quantity $Z^{-1/2}$ has a clear geometrical interpretation: it is the length, with an inverse mass metric, of the component of the vector $\partial \phi / \partial \mathbf{r}$ orthogonal to the space spanned by the molecular constraint vector $\partial \sigma / \partial \mathbf{r}$. That is [3]

$$Z = \sum_{i=1}^N \frac{1}{m_i} \left(\frac{\partial \phi}{\partial \mathbf{r}_i} \right)^2 \quad (59)$$

For the elementary example of a reaction coordinate consisting only of a distance between two atoms i and j , $\phi = |\mathbf{r}_i - \mathbf{r}_j|$, $G = 0$ and Z is the constant value $Z = \mu^{-1}$, where μ is the reduced mass of both atoms. Hence, the mean force can be estimated directly from the time average of the Lagrange multiplier over the constrained MD trajectory without the need for reweighting or correction terms.

The probability density of finding the system in any point of the configuration space such that $\phi(\mathbf{r}) = \phi'$ is [5]

$$P(\phi(\mathbf{r}) = \phi') = \langle \delta(\phi(\mathbf{r}) = \phi') \rangle \equiv C e^{-A(\phi')/k_B T}, \quad (60)$$

where $\langle \dots \rangle$ is the ensemble average. The constant C is determined by the normalization condition on $P(\phi)$.

The free energy difference can be thought of as the work necessary to change the system from the initial to final state. Since the free energy A is a state function, ϕ can represent any pathway, even non-physical pathways. However, if ϕ is chosen to be a reaction coordinate as to represent a physical reaction path, the procedure determines an upper bound for a reaction free energy barrier by means of thermodynamic integration.

The conceptual advantage of the free energy integration is that the entropy is explicitly included in the reaction barrier. Another important advantage is that the phase space is explored more effectively than by using the zero-temperature transition state search. Hence, in many cases unexpected reaction mechanisms become evident that would have been missed in the more controlled zero-temperature regime. The free energy integration has been generalized to solvated systems.

TABLE I: Parameters for constraint MD simulations taken from the literature (NH – Nosé Hoover thermostat, NHC – NH chain thermostat, SG – slow growth, incr – incremental).

type	RC	RC length	δt [fs]	t_{eq} [ps]	t_{prod} [ps]	T [K]
sg ^{a)}	dist	1.50 Å	~ 4.1	–	4.84	300 (NH)
sg ^{a)}	dist	1.80 Å	~ 4.1	–	4.84	300 (NH)
sg ^{a)}	dist	1.44 Å	~ 4.1	–	6.65	300 (NH)
incr ^{b)}	S_N2 ^{c)}	0–1	0.19	1.5–3/incr	3–5/incr	300 (NHC)
incr ^{e)}	ddist	-0.5–0.7	0.17	–	1.5–2.5/incr	300 (NH)
incr ^{f)}	dist	1.3 Å	0.34	2	1.5–2.5/incr	300 (NH)

- ^{a)} Margl, Ziegler and Blöchl *J. Am. Chem. Soc.* **118**, 5412 (1996).
^{b)} Ensing, Meijer, Blöchl and Bearends *J. Phys. Chem. A* **105**, 3300 (2001). ^{c)} $\zeta = |\mathbf{r}_{21}| \cos(\angle_{123}) / |\mathbf{r}_{13}|$. ^{d)} After each production run the constraint was moved to the next RC value in a number of steps large enough to keep the induced atomic velocities very small compared to their average velocities (typically 1000–2000 steps).
^{e)} Meijer and Sprik *J. Am. Chem. Soc.* **120**, 6345 (1998). ^{f)} Curioni, Sprik, Andreoni, Schiffer, Hutter and Parrinello *J. Am. Chem. Soc.* **119**, 7218 (1997).

The reaction coordinate ϕ can be sampled discretely or carried out in a continuous manner in what is termed a “slow growth”. The discrete sampling resembles a linear transit calculation such that a series of simulations is set up corresponding to successive values of the reaction coordinate from the initial to final state. The free energy is calculated with

$$\Delta A = \sum_{i=1}^{N_{steps}} F(\phi_i) \Delta \phi_i, \quad (61)$$

where N_{steps} indicates the discretisation. For each sample point the dynamics must be run long enough to achieve an adequate ensemble average of the mean force on the fixed reaction coordinate.

In a “slow growth” simulation the reaction coordinate is continuously varied throughout the dynamics from the initial to the final state. Thus, in each time step the reaction coordinate is incrementally changed from that in the previous time step. Hence, the system is never properly equilibrated unless the change in the reaction coordinate is infinitesimally small (reversible change). However, the smaller the rate of change the better the approximation. Since the reaction coordinate is changed at each time step the force on the reaction coordinate is biased depending on the direction in which the reaction coordinate is varied. Therefore, a forward and reverse scan of the reaction coordinate is likely to give different results. This is a direct consequence of the improper equilibration. Thus it is generally a good idea to perform both forward and reverse scans to reduce this error and to determine whether the rate of change of the reaction coordinate is appropriate. The advantage of “slow growth” simulations is that the dynamics is not disrupted when the reaction coordinate is changed and, hence, the system only has to be thermally equilibrated once. On the other hand the method has the disadvantage that both the forward and reverse scans should be performed.

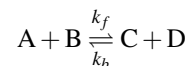
A simple and reliable way to estimate the change in free energy for dissociation of a weak acid (A) is given by the following equations[11]:

$$\Delta A = \Delta A^0 + 2.303RT \log \frac{[A^-][H^+]}{[AH]} \quad (62)$$

$$\Delta A^0 = 2.303RT pK_a \quad (63)$$

XI. TRANSITION STATE THEORY

The rate constants and their temperature dependence allow the computation of reaction progress over a range of temperatures. If the *forward* and *backward* rate constants k_f and k_b are known for the reaction



then the equilibrium constant K_{eq} for that elementary reaction can be calculated as well, for [8]

$$K_{eq}(T) = \frac{k_f(T)}{k_b(T)}, \quad (64)$$

where (T) is used to emphasize the temperature dependence. Note that this enables the direct calculation of the equilibrium isotope fractionation factors for overall reactions. In addition to knowing the rates of the reactions *per se* and calculating equilibrium constants for elementary reactions, knowledge of the thermal rate constants allows the prediction of phenomena such as kinetic isotope effects (KIE). For instance, the primary KIE of an elementary reaction may be evaluated using [8]

$$\text{KIE}(T) = \frac{k_f^*(T)}{k_f(T)} \quad (65)$$

assuming that the isotope is directly involved in the reaction and where the star indicates the same reaction but with different isotope signature.

Classical transition state theory (TST) provides a formalism for predicting thermal rate constants by combining the important features of the potential energy surface (PES) with a statistical representation of the dynamics of the system. One of the fundamental assumptions of TST is that there exists a divide in the PES that separates the reactant and product regions. This divide contains the transition state, AB^\ddagger , which is defined as the maximum value in the minimum energy path of the PES that connects the reactant (AB) and the product (CD). The transition state is characterized by the rarest value of the reaction coordinate, $\phi(\mathbf{r}) = \phi^\ddagger$. The reactant and product sides of the free energy profile are defined by those states with $\phi(\mathbf{r}) < \phi^\ddagger$ and $\phi(\mathbf{r}) > \phi^\ddagger$, respectively. The probability of finding the system, e.g., on the reactant side is given by the equilibrium average of the population function

$$n_{AB} = \Theta(\phi^\ddagger - \phi) = \begin{cases} 1 & \phi \leq \phi^\ddagger \text{ (reactant side)} \\ 0 & \phi > \phi^\ddagger \text{ (product side)} \end{cases} \quad (66)$$

where $\Theta(\phi^\ddagger - \phi)$ is the Heaviside step function. The equilibrium average of the population function $n_{CD} = \Theta(\phi - \phi^\ddagger)$ yield the probability of finding the system on the product side. Both population functions have the properties [14]

$$n_{AB} + n_{CD} = 1, n_{AB}^2 = n_{AB}, n_{AB}n_{CD} = 0.$$

However, n_{AB} and n_{CD} are equal to step functions outside the barrier region because the barrier region contributes negligibly to equilibrium averages. The time derivative of the population function n_{AB} , $\dot{\Theta}(\phi^\ddagger - \phi) = \dot{\phi}\delta(\phi^\ddagger - \phi)$, is the microscopic expression for its flux, where $\dot{\phi}$ is the reaction coordinate velocity [4].

Within the TST it is assumed that every trajectory passing through the transition state from the reactant side is assumed to form products eventually. The latter is known as the ‘‘non-crossing rule’’ is the reason why TST yields an upper bound to the true rate constant [13].

If τ_{TS} is defined to be the average lifetime of the transition state (TS) in the reaction $A + B \rightleftharpoons AB^\ddagger \rightarrow C + D$ and each transition state complex is assumed to turn to products then the concentration change per unit time of the particles is [8]

$$k_f^{TST}(T) = \frac{[AB^\ddagger]}{\tau_{TS}(T)[A][B]} = \frac{K^\ddagger(T)}{\tau_{TS}(T)} = v^\ddagger(T)K^\ddagger(T), \quad (67)$$

where $v^\ddagger = 1/\tau_{TS}$ is the (imaginary) vibrational frequency of conversion of AB^\ddagger to the products. The assumption that the reactant and transition state are in equilibrium with each other leads to the formulation of a quasi-equilibrium constant $K^\ddagger(T)$. The equilibrium assumption also leads to the use of quasi-thermodynamic extensive variables that are treated as if they were true thermodynamics values.

If all species i are treated as ideal gases and the quasi-equilibrium constant is represented in terms of molecular partition functions, q_i , the *forward* rate constant can be formulated as[8]

$$k_f^{TST} = \frac{k_B T}{h} \frac{(q^\ddagger/V)}{(q_A/V)(q_B/V)} e^{-\Delta\epsilon_0/k_B T} \quad (68)$$

where q^\ddagger , q_A and q_B are the molecular partition functions of the transition state and the reactant(s), respectively, h is Planck’s constant, and $\Delta\epsilon_0$ is the difference in the zero-point vibrational energies between the reactant(s) and the transition state. The partition function q^\ddagger involves the partition function of AB^\ddagger but without the (imaginary) vibrational frequency, v^\ddagger . The latter is included as translational degree of freedom in the term $k_B T/h$ of Eq. (68).[21] Hence, the rate constant of a given elementary reaction can be calculated when the E_{ZPE} and the partition functions of the reactant(s) and the transition state are known. The rate constants calculated for reactions in the liquid phase are valid if the transfer of energy into the system and the transport of the reactant(s) into the reaction zone are not rate limiting.

The molecular partition function of a species i may be separated into its molecular, translational, vibrational, electronic and nuclear partition functions

$$q_i = q_{i,trans} q_{i,rot} q_{i,vib} q_{i,elec} q_{i,nuc}. \quad (69)$$

The translational partition function is given by

$$q_{i,trans} = \left(\frac{2\pi m_i k T}{h^2} \right)^{3/2} V, \quad (70)$$

where m_i is the mass of the species i . The quantity V is the volume and need not be known because it is eventually canceled by the volume in the rate constant equation (68).

The rotational partition function depends on the shape of the molecule. For a linear molecule the partition function is

$$q_{i,rot} = \frac{8\pi^2 I k T}{\sigma h^2}, \quad (71)$$

where I is the moment of inertia and σ is the symmetry number. The latter is the number of different ways the molecule can rotate into a configuration indistinguishable from the original. For a non-linear molecule the partition function is

$$q_{i,rot} = \frac{\sqrt{\pi}}{\sigma} \left(\frac{8\pi^2 I_x k T}{h^2} \right)^{1/2} \left(\frac{8\pi^2 I_y k T}{h^2} \right)^{1/2} \left(\frac{8\pi^2 I_z k T}{h^2} \right)^{1/2}, \quad (72)$$

where I_k ($k = x, y, z$) are the three principal moments of inertia corresponding to the three principal rotational modes.

The vibrational partition function relative to E_{ZPE} is a function of the vibrational frequencies ν for each vibrational mode j ,

$$q_{i,vib} = \prod_{j=1}^a \frac{1}{(1 - e^{-h\nu_j/kT})}. \quad (73)$$

Note, that the neglect of E_{ZPE} is a common error in an evaluation of reaction feasibility. While energy differences where E_{ZPE} is not considered are occasionally helpful in quantitatively determining whether the hypothesized reaction produces the expected rate. The zero-point vibrational energy should unequivocally be considered in any quantitative TST evaluation of reaction rates.

The nuclear partition function is a Boltzmann-weighted sum of the degeneracy of each nuclear state. In general, only the first term is relevant because the energy differences between the states are extremely large and transitions between different states does not normally occur in chemical reactions:

$$q_{i,nuc} = \sum \omega_{nj} e^{-\epsilon_{nj}/kT} = \omega_{n1} e^{-\epsilon_{n1}/kT}. \quad (74)$$

In Eq. 74, ω_{nj} is the degeneracy of the nuclear state j and ϵ_{nj} is the corresponding nuclear energy. If the nuclear ground state is used as reference ($\epsilon_{n1} = 0$) then $q_{i,nuc}$ only contributes as multiplicative constant to q_i , specifically ω_{n1} . Because the nuclear states in general do not change as the system goes from reactant(s) to transition state, $q_{i,nuc}$ can be assumed as unity in Eq. (69).

Similar to the nuclear partition function, the electronic partition function is a Boltzmann-weighted sum of the degeneracy of each electronic state:

$$q_{i,elec} = \sum \omega_{ej} e^{-\epsilon_{ej}/kT}, \quad (75)$$

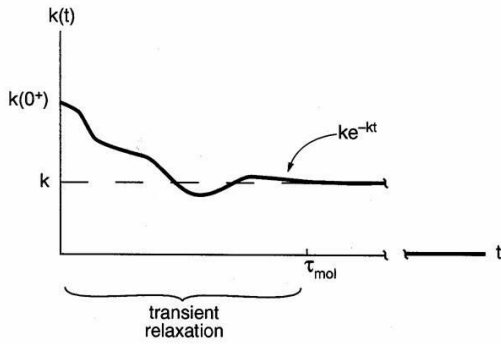


FIG. 1: Reactive flux correlation function. After the transient relaxation, $k(t)$ relaxes exponentially, as $k \exp(-kt)$, where $k^{-1} \gg \tau_{mol}$ and τ_{mol} is the order of a typical microscopic relaxation time. This figure is adapted from Ref. [4].

where ω_{ej} is the degeneracy of the electronic state j and ϵ_{ej} is the corresponding electronic energy. The first term in the sum involves the electronic ground state energy ($j = 0$) and the succeeding terms are excited energy levels.

The TST rate constant calculated within the 'blue moon ensemble' is defined as [3]

$$k_f^{TST} = \sqrt{\frac{k_B T}{2\pi}} \langle Z^{-1/2} \rangle_{\phi^\ddagger} \frac{\langle \delta(\phi - \phi^\ddagger) \rangle}{\langle \Theta(\phi^\ddagger - \phi) \rangle}. \quad (76)$$

The ensemble average of the Kronecker delta function in Eq. (76), $\delta(\phi - \phi^\ddagger)$, is equivalent to the probability density of the reaction coordinate at $\phi = \phi^\ddagger$, $\langle \delta(\phi - \phi^\ddagger) \rangle = P(\phi^\ddagger)$ [Eq. (60)]. The denominator of Eq. (76), is the integral of the probability density of the reaction coordinate over the well of the reactant side [5]:

$$\langle \Theta(\phi^\ddagger - \phi) \rangle = \int_{\phi' < \phi^\ddagger} d\phi' \langle \delta(\phi - \phi') \rangle = \int_{\phi' < \phi^\ddagger} P(\phi') d\phi'. \quad (77)$$

The overall form of the right hand-side of Eq. (76) can be (approximately) understood from each term [17]. The first two terms identify an average velocity of the atoms involved in the reaction coordinate at the TS and the integral in the denominator of the third term is a measure of the width of that well of A + B. Thus, the width/velocity leads to a frequency factor that is the number of attempts made by the system to leave the well. A broader well leads to a larger value of the denominator and thus a lower rate constant. Finally, the term in the numerator describes the probability of success of a given attempt to pass over the activation free energy barrier and is a depends on the height of the free energy barrier.

XII. CORRECTIONS TO THE TRANSITION STATE THEORY

A. Barrier recrossing

Transition state theory provides rate constants for processes where a system in the well of the reactant side reaches the barrier a ϕ^\ddagger and forms products eventually. However, particular interaction can cause a recrossing of the free energy barrier back to the reactant side leading to lower values of the kinetic rate constant. To account for this dynamical effect, the rate constant k_f is defined in terms of the TST rate constant k_f^{TST} and the transmission coefficient κ [3–5, 15]

$$k_f = k_f^{TST} \kappa. \quad (78)$$

The transmission coefficient, $0 \leq \kappa \leq 1$, is the average flow of trajectories passing through the transition state and succeed in crossing the barrier at time t given that the system was at the transition state at time zero. Ref. [20] provides an overview and survey of algorithms to calculate transmission coefficients.

One algorithm which is related the blue moon ensemble to compute the transmission coefficient was introduced by Berne and co-workers (see Refs. [3, 5, 20] for more details). The transmission coefficient is given by the correlation function

$$\kappa(t) = \frac{\langle Z^{-1/2} \dot{\phi}(0) \Theta(\dot{\phi}(0)) \delta(\phi(0) - \phi^\ddagger) \Theta(\phi(t) - \phi^\ddagger) \rangle}{\langle Z^{-1/2} \dot{\phi}(0) \Theta(\dot{\phi}(0)) \delta(\phi(0) - \phi^\ddagger) \rangle}, \quad (79)$$

where $\Theta(\dot{\phi}(0))$ is 1 or 0 for $\dot{\phi}(0) > 0$ and $\dot{\phi}(0) < 0$, respectively, at time $t = 0$. To determine κ , the real dynamics and not the constrained dynamics of a system has to be known [5]. The transmission coefficient κ is accessible by calculating the correlation function in Eq. (79) from n independent and unconstrained MD simulations starting from states with $\phi = \phi^\ddagger$ at $t = 0$. The start configurations for the unconstrained MD simulations are generated from simulations in which the constraints $\phi = \phi^\ddagger$ and $\dot{\phi} = 0$ were applied. It has to be ensured that the n atomic start configurations are uncorrelated. The initial atomic velocities are generated in accordance with the Maxwell-Boltzmann distribution. Starting from the random velocity configurations, n unconstrained MD simulations are performed for, e.g., 800 time steps. For example, Forester and Smith [9] generated 220 separated start configurations for the unconstrained MD simulations.

In each of the n MD simulations, $\kappa(t)$ converges to a certain value, κ (Fig. 1), for times that are 'long' on the timescale of barrier crossing ($\kappa = \lim_{t \rightarrow \infty} \kappa(t)$), but 'short' on the timescale of the activated processes. The overall value of κ is obtained by taking average over the n different trajectories: $\kappa = 1/n \sum_{i=1}^n \kappa_i$. The oscillations of $\kappa(t)$ during its evolution correspond to recrossing events[9].

One simple algorithm requires computing the particle motion only until the system of interest recrosses the barrier top:

$$\kappa = \frac{n_{\phi^\ddagger \rightarrow \phi^{prod}}}{n}, \quad (80)$$

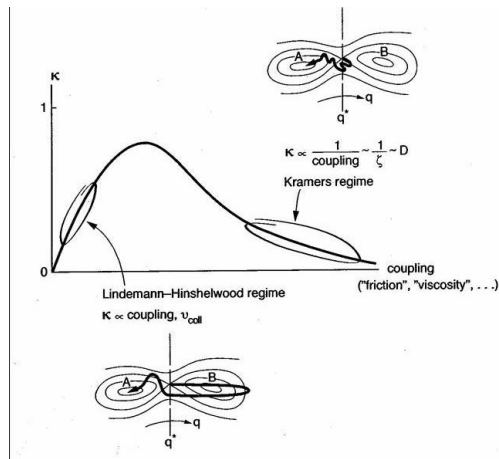


FIG. 2: Variation of the transmission coefficient, κ , as a function of the coupling between a reaction coordinate and a bath. “Coupling” refers to the rate at which energy can flow from the reaction coordinate to other degrees of freedom. Depending upon the physical situation, it could be proportional to a “collision frequency”, “friction” or “viscosity”, ζ , or the reciprocal of the spatial diffusion constant, D^{-1} . This figure is adapted from Ref. [4].

where where $n_{\phi^\ddagger \rightarrow \phi^{prod}}$ is the number of trajectories starting at the transition state proceeding directly to product and originating as reactant, i.e. $\dot{\phi}(0) > 0$ and $\Theta(\phi(t) - \phi^\ddagger) = 1$ for each t . Equation (80) is the Anderson algorithm. The transmission coefficient κ is accessible from n independent and unconstrained MD simulations starting from states with $\phi = \phi^\ddagger$. The start configurations for the unconstrained MD simulations are generated from simulations in which the constraints $\phi = \phi^\ddagger$ and $\dot{\phi} = 0$ were applied. It has to be ensured that the n atomic start configurations are uncorrelated. The initial atomic velocities are generated in accordance with the Maxwell-Boltzmann distribution. Starting from the random velocity configurations, n unconstrained MD simulations are performed for, e.g., 800 time steps. Only those trajectories are counted which proceed directly to product and which, when followed backward in time, originate as reactant. Due to its simplicity and low uncertainty in κ ($\sim 15\%$) the Anderson algorithm is strongly recommended [20].

However, when $\kappa \ll 1$ the expression for the reactive flux obtained from Eq. (79) is, although correct, not the best starting point for a computer simulation [14]. In the calculation of κ , a set of trajectories in which the system is put initially in the transition state and its posterior evolution is followed until the plateau is reached (Fig. 1). The statistical error in κ is given by [14]

$$\frac{\sigma_\kappa}{\kappa} \sim \frac{1}{\kappa\sqrt{n}}. \quad (81)$$

If the transmission coefficient is of the order of 0.1, then about 10^4 trajectories have to be considered to get a 10% accuracy. Moreover, the smaller the transmission coefficient the more trajectories have to be considered to get a reasonable estimate for the rate.

Another but similar approach which takes recrossing effects into account is that of Grote and Hynes [10, 17]. Here, the rate constants is the product of k_f^{TST} and the Grote-Hynes transmission coefficient κ^{GH} . The latter depends on the autocorrelation function of the forces between the reactants along the reaction coordinate ϕ :

$$\kappa^{GH} = \left[\kappa^{GH} + \omega_b^{-1} \int_0^\infty \delta t \exp(-\kappa^{GH} \omega_b t) \zeta(t, \phi^\ddagger) \right]^{-1} \quad (82)$$

$$\zeta(t, \phi^\ddagger) = \frac{1}{\mu k_B T} \frac{\langle F(t, \phi^\ddagger) F(t=0, \phi^\ddagger) \rangle}{\langle F(t, \phi^\ddagger)^2 \rangle} \quad (83)$$

In Eq. (82), $F(t, \phi^\ddagger)$ is the mean force due to structural constraint [Eq. (57)], and ω_b is the barrier frequency which is related to the sharpness of the peak of the energy barrier. The barrier frequency is found by fitting the free energy profile at the peak of the barrier with the parabola defined by

$$A(\phi) = -\frac{1}{2} \mu (2\pi\omega_b)^2 \phi^2.$$

B. Quantum tunneling corrections

Quantum tunneling occurs when a configuration that has an energy lower than an energy barrier nonetheless surmounts it due to quantum mechanical effects. In such cases, adjustments of the rate constant due to tunneling become necessary to obtain improved accuracy. These corrections in TST are in the form of a correction coefficient κ such that [8]

$$k_r^{un} = \kappa k_r^{TST}, \quad (84)$$

where $k_{r,corr}$ is the corrected rate constant. In the Wigner treatment which is the most common correction made, the correction coefficient is given as

$$\kappa = 1 + \left| \frac{\hbar v^\ddagger}{2\pi k_B T} \right|^2, \quad (85)$$

where v^\ddagger is the imaginary vibrational frequency at the saddle point. However, this correction is only valid if certain conditions are satisfied. The contributions to tunneling must only come from the saddle point region of the PES where transverse modes do not vary appreciably. The PES curvature should be that of a concave down parabola. The Wigner correction is considered valid only at very high temperatures where it is near unity.

XIII. THERMODYNAMIC ASPECTS

A system L is composed of a system of interest, L_1 , which is in thermal equilibrium with a heat reservoir, L_2 , at temperature T . In principle, A is closed so that the total internal energy remains constant. Then, at a certain instant the system is opened and an external work source is invoked which

performs reversible work on A_1 at an adiabatic rate without exchanging any heat. How do the internal energies (U_1, U_2), entropies (S_1, S_2), and Helmholtz free energies (A_1, A_2) of L_1 and L_2 change during this adiabatic isothermal process? The change of these quantities is considered due to an infinitesimal amount of work dW done on L_1 . According to the first law of thermodynamics

$$dU_1 = TdS_1 + dW \quad (86)$$

$$dU_2 = TdS_2 \quad (87)$$

The heat reservoir cannot perform any work. Furthermore, since the process is adiabatic, the total entropy change satisfies

$$dS = dS_1 + dS_2 = 0 \quad (88)$$

The changes in the Helmholtz free energies of the subsystems L_1 and L_2 are

$$dA_1 = dU_1 - TdS_1 \quad (89)$$

$$dA_2 = dU_2 - TdS_2 \quad (90)$$

The Helmholtz free energy change of the heat reservoir satisfies $dF_2 = 0$ as can be seen from Eqs. (87) and (90). Inserting this information and Eq. (88) into the sum of Eqs. (89) and (90) one yields

$$dA_1 = dU_1 + dU_2 \quad (91)$$

Thus the change of the Helmholtz free energy of subsystem L_1 is equal to the change of the total internal energy of

the composite system L . For the complete process, the total Helmholtz free energy change of the physical system will be $\Delta A_1 = \Delta U_1 + \Delta U_2$. This is exactly the same result as derived by Watanabe and Reinhardt for adiabatic switching procedures using Nosé dynamics (see Ref. [6]). This agreement seems reasonable since the dynamics of these procedures contains all microscopic elements necessary to fulfill the macroscopic thermodynamic conditions of the analysis above. First of all, the thermostat subsystem of the Nosé dynamics maintains the physical system and itself at a constant temperature. This is accomplished exclusively by exchanging heat. The thermostat system cannot perform any work since no external parameters are present in its equations of motion. Secondly, the Nosé dynamics conserves the total energy of the extended system closed. Finally, the adiabatic reversible work done by the external source is represented by a coupling parameter λ which varies very slowly in time. Clearly, the external work is done without any heat exchange since the only link between the physical system and the work source is the parameter λ .

Adiabatic switching processes that use the massive Nosé-Hoover chain (MNHC) dynamics, have equations of motions compatible with the macroscopic conditions of the Nosé dynamics. Therefore, adiabatic switching procedures combined with MNHC dynamics represent adiabatic isothermal processes in the thermodynamic sense and can be used to determine Helmholtz free energies by applying Eq. (91).

-
- [1] P. W. Atkins, *Physical chemistry*, Oxford University Press, New York, 1990.
- [2] P. E. Blöchl, H. M. Senn, and A. Togni, *Molecular reaction modeling from ab-initio molecular dynamics*, Transition State Modeling for Catalysis (D. G. Truhlar and K. Morokuma, eds.), ACS Symposium Series, vol. 721, American Chemical Society, Washington, 1999, p. 88.
- [3] E. A. Carter, G. Ciccotti, J. T. Hynes, and R. Kapral, *Constrained reaction coordinate dynamics for the simulation of rare events*, Chem. Phys. Lett. **156** (1989), no. 5, 472.
- [4] D. Chandler, *Barrier crossings: classical theory of rare but important events*, Classical and quantum dynamics in condensed phase simulations (B. Berne, G. Ciccotti, and D. F. Coker, eds.), World Scientific, Singapore, 1998, p. 3.
- [5] G. Ciccotti and M. Ferrario, *Rare events by constrained molecular dynamics*, J. Mol. Liquids **89** (2000), 1.
- [6] M. de Koning and A. Antonelli, *Einstein crystal as a reference system in free energy estimation using adiabatic switching*, Phys. Rev. E **53** (1996), no. 1, 465.
- [7] B. Ensing, E. J. Meijer, P. E. Blöchl, and E. J. Baerends, *Solvation effects on the $s_{\text{r}}2$ reaction between ch_3cl and cl^- in water*, J. Phys. Chem. A **105** (2001), no. 13, 3300.
- [8] M. A. Felipe, Y. Xiao, and J. D. Kubicki, *Molecular orbital modeling and transition state theory in geochemistry*, Reviews in Mineralogy and Geochemistry (R. T. Cygan and D. Kubicki, eds.), vol. 42, The Mineralogical Society of America, 2001, p. 485.
- [9] T. R. Forester and W. Smith, *Bluemoon simulations of benzene in silicate-1. prediction of free energies and diffusion coefficients*, J. Chem. Soc., Faraday Trans. **93** (1997), no. 17, 3249.
- [10] R. F. Grote and J. T. Hynes, *The stable states picture of chemical reactions. ii. rate constants for condensed and gas phase reaction models*, J. Chem. Phys. **73** (1980), no. 6, 2715.
- [11] I. Ivanov and M. L. Klein, *Deprotonation of a histidine residue in aqueous solution using constrained ab initio molecular dynamics*, J. Am. Chem. Soc. **124** (2002), no. 45, 13380.
- [12] R. Kutteh and T. P. Straatsma, *Molecular dynamics with general holonomic constraints and application to internal coordinate constraints*, Reviews in Computational Chemistry (K. B. Lipkowitz and D. B. Boyd, eds.), vol. 12, Wiley-VCH, New York, 1998, p. 75.
- [13] A. Luzar, *Resolving the hydrogen bond dynamics conundrum*, J. Chem. Phys. **113** (2000), no. 23, 10663.
- [14] M. J. Ruiz-Montero, *From eyring to kramers: computation of diffusive barrier crossing rates*, Classical and quantum dynamics in condensed phase simulations (B. J. Berne, G. Ciccotti, and D. F. Coker, eds.), World Scientific, Singapore, 1998.
- [15] M. J. Ruiz-Montero, D. Frenkel, and J. J. Brey, *Efficient schemes to compute diffusive barrier crossing rates*, Mol. Phys. **90** (1997), no. 6, 925.
- [16] J.-P. Ryckaert, G. Ariedi, and S. Melchionna, *Molecular dynamics of polymers with explicit but frozen hydrogens*, Mol.

- Phys. **99** (2001), no. 3, 155.
- [17] J. Y. Shin and N. L. Abbott, *Combining molecular dynamics simulations and transition state theory to evaluate the sorption rate constants for decanol at the surface of water*, *Langmuir* **17** (2001), 8434.
- [18] J. T. Slusher and P. T. Cummings, *Non-iterative constraint dynamics using velocity explicit verlet methods*, *Molec. Sim.* **18** (1996), 213.
- [19] M. Sprik and G. Ciccotti, *free energy from constrained molecular dynamics*, *J. Chem. Phys.* **109** (1998), no. 18, 7737.
- [20] G. W. N. White, S. Goldman, and C. G. Gray, *Test of rate theory transmission coefficient algorithms. an application to ion channels*, *Mol. Phys.* **98** (2000), no. 22, 1871.
- [21] The partition function of v^\ddagger is $1/(1 - \exp[-hv^\ddagger/k_B T])$. Usually, the vibrational frequency v^\ddagger is much smaller than the other vibrational frequencies of a, e.g., molecule. If $-hv^\ddagger/k_B T \ll 1$ then the exponential function can be expanded in series and the partition function of v^\ddagger is equivalent to $k_B T/(hv^\ddagger)$.